We are IntechOpen, the world's leading publisher of Open Access books Built by scientists, for scientists

6,900
Open access books available

185,000
International authors and editors

200M
Downloads

Our authors are among the

154
Countries delivered to

TOP 1%
most cited scientists

12.2%
Contributors from top 500 universities



WEB OF SCIENCE™

Selection of our books indexed in the Book Citation Index in Web of Science™ Core Collection (BKCI)

Interested in publishing with us?
Contact book.department@intechopen.com

Numbers displayed above are based on latest data collected.
For more information visit www.intechopen.com



Chapter 3

Polymeric Additive Manufacturing: The Necessity and Utility of Rheology

Mohammed Elbadawi

Additional information is available at the end of the chapter

http://dx.doi.org/10.5772/intechopen.77074

Abstract

Additive manufacturing techniques have recently seen an explosive growth across a myriad of fields, partly galvanised by their advantages over traditional fabrication techniques. As with most fabrication processes, maximising efficiency is a requisite, particularly if commercialisation is sought-after. Understanding how the material behaves during additive manufacturing is necessary to accomplishing said task. Accordingly, the chapter herein collates examples of where rheology is applicable in polymer-based additive manufacturing techniques, thereby demonstrating the necessity and utility thereto. The main focus herein will be fused deposition modelling and stereolithography additive manufacturing techniques, with examples of how both capillary and rotational rheometers can be utilised.

Keywords: additive manufacturing, 3D printing, fused deposition modelling, stereolithography, rheology

1. Introduction

Additive manufacturing (AM), also referred to as solid freeform fabrication, rapid prototyping and three-dimensional (3D) printing, is ostensibly a transformative manufacturing technique that will play a vital role in the next Industrial Revolution. AM entails the fabrication of 3D structures with both geometrical complexities and spatial resolution beyond the capacity of traditional fabrication techniques. The ubiquity of AM, from the automotive and aerospace industry, to tissue engineering and drug delivery, unequivocally demonstrates the rising appeal of the technology. From a research perspective, AM allows for rapid prototyping and integration with other technologies, that again, seldom observed in traditional routes.

IntechOpen

© 2018 The Author(s). Licensee IntechOpen. This chapter is distributed under the terms of the Creative Commons Attribution License (http://creativecommons.org/licenses/by/3.0), which permits unrestricted use, distribution, and reproduction in any medium, provided the original work is properly cited. CC BY

Furthermore, there are several polymeric AM technologies available for purchase by consumers that will allow manufacturing of goods to be achieved at home. However, despite the vast progression made, the technology is still in its infancy. Therefore, to make AM an essential instrument, further research is needed, including new material formulations.

Rheology is a necessity for all polymer fabrication techniques. The characterisation can deliver extensive and reliable material information. The data is subsequently correlated to the process to maximise productivity. Rheology will further be a key component as new materials are formulated to advance the versatility of AM. In spite of this, rheology remains an underutilised tool. Thus, a chapter into how rheology can be utilised to help maximise AM efficiency is warranted. The chapter presents two of the commonly-used AM techniques in the field of polymers: fused deposition modelling (FDM) and stereolithography (SLA); and demonstrates the necessity of rheology thereto. As detailed herein, both technologies form 3D structures through disparate means, and albeit different, rheology is still an indispensable tool for both technologies. The chapter will conclude with a brief description of other AM techniques and how rheology is still relevant.

2. Fused deposition modelling

Fused deposition modelling (FDM) is one of the most common polymer additive manufacturing techniques. FDM is an extension of hot melt extrusion (HME), which is an already established technique in the field, whereby thermoplastics are heated to their semi-molten state and extruded through a given orifice. However, HME can only be used to fabricate basic geometries, whereas FDM utilises a gantry system that allows a nozzle to move and extrude the semi-molten polymer in three-dimensions until a 3D print is fabricated.

The similarities between FDM and HME are that both use high heat to achieve a semi-molten thermoplastic polymer, and that it is then forced through an orifice[1]. Hence, high temperature rheology and the shearing effect at the orifice, respectively, are of interest to both. Upon exiting the orifice, the thermoplastic is cooled until solidification, which again, is rheologically relevant. The rheological events of FDM are delineated in **Figure 1**.

2.1. Nozzle flow and viscosity

2.1.1. Determining the shear rate from FDM parameters

Knowing the ideal viscosity range can help in predicting whether the new melt formulation is extrudable. Said knowledge will prevent time-consuming and costly empirical trials, as well as mitigating nozzle blockage and consequently machine downtime. A straightforward approach is to compare the viscosity of the new formulation to that of a successfully extruded formulation (e.g. a commercial filament) using a rheometer. A dissimilar viscosity profile may not necessarily equate to an unextrudable melt, provided that they possess comparable viscosity at the operating shear rate; hence the shear rate of interest will need to be identified. Unlike HMEs,

[1]For HME, the orifice is typically called a die; for FDM it is the nozzle.

http://dx.doi.org/10.5772/intechopen.77074

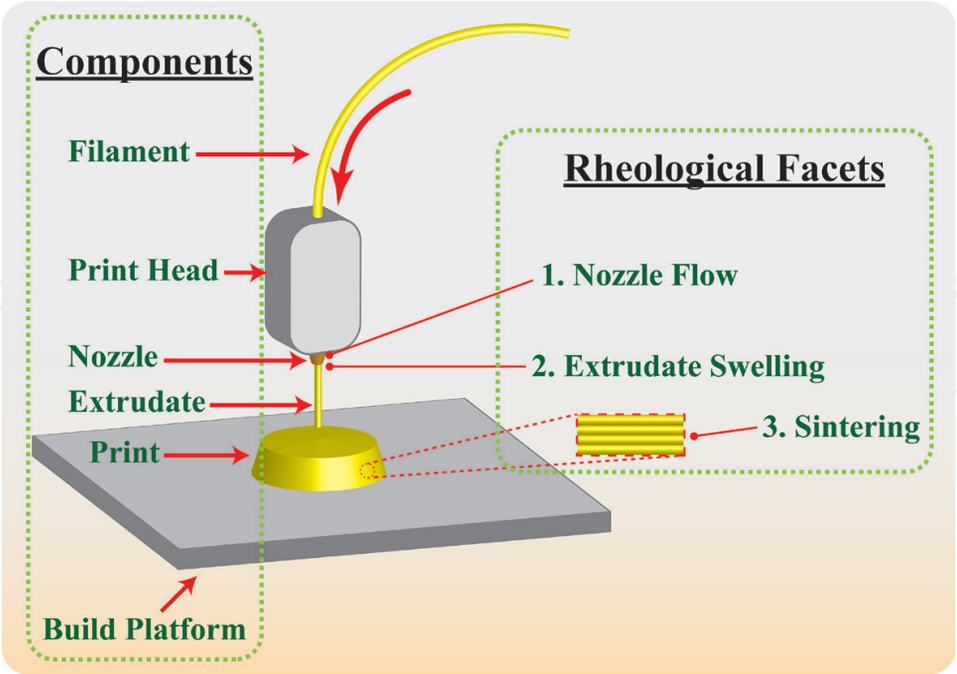


Figure 1. Schematic of fused deposition modelling. The figure lists the components involved in the fabrication process, as well as the rheological facets of interest measurable by rheometers.

however, most FDMs are not equipped with a transducer, and thus the shear rate will need to be determined semi-empirically. This can be achieved by: (i) performing an initial shear-rate viscosity measurement of the melt to obtain the power law index; (ii) knowing the speed of printing and nozzle diameter; and (iii) applying the rheological equations (Eqs. (1)–(4)).

The apparent shear rate $\dot{\gamma}_{app}$ of the nozzle can be semi-empirically determined using the following equation [1]:

$$\dot{\gamma}_{app} = \frac{4Q}{\pi r^3} \tag{1}$$

where Q is the volume flow rate, determined from the exit nozzle radius r and the speed of extrusion v (i.e. printing speed) [1]:

$$Q = \pi r^2 v \tag{2}$$

For example, a printing speed of 50 mm/s and a nozzle diameter of 0.2 mm equates to a flow rate of 6.3 mm^3/s and consequently an apparent shear rate of ~1000 s^{-1}. The apparent shear rate $\dot{\gamma}_{app}$ provides a relatable shear rate that is then examined using the rheometer, which is typically in the order of 10^2 to 10^3 s^{-1} [2]. Thus, a capillary rheometer is best suited for such analysis, as 10^3 s^{-1} is above the attainable shear rate performed by a rotational rheometer [3]. For the true shear rate $\dot{\gamma}$, the following equation should be used [4–6]:

$$\dot{\gamma} = \dot{\gamma}_{app}\left(\frac{(3n+1)}{4n}\right) \tag{3}$$

whereby n is the power law index obtained using the power law model from a viscosity-shear rate test:

$$\eta = k\dot{\gamma}^{n-1} \tag{4}$$

The best fit[2] to the data gives the power law index n, which is a dimensionless value between 0 and 1[3]. From the above equations, the true shear rate at the nozzle wall can be obtained, and therefore, viscosity-shear rate tests can be performed at the relatable shear rate range.

Although a capillary rheometer covers the ideal shear rate found in FDM, and exhibits the same flow behaviour to that found within the nozzle (i.e. Poiseuille flow), a rotational rheometer can be used if a capillary rheometer is not accessible. A shear rate test can be performed up to the instrument's shear rate limit, and the experimental data can then be fitted with a rheological model to predict the viscosity at higher shear rates. Examples of curve fitting models include the power law model, Williamson model, Cross model and Carreau-Yasuda model. Note that the oscillatory mode extends the shear rate limit of the rotational mode, however, the former provides the complex viscosity. If the Cox-Merz rule [7] is upheld for the melt formulation, then the complex viscosity can be converted into the steady-state viscosity, and subsequently curve fitted.

In addition to the above rotational rheometer analysis, large amplitude oscillatory shear (LAOS) measurements can be conducted to investigate the performance of the formulation. LOAS is regarded as a more complex analysis, however, it can be more revealing than its counterparts: small amplitude oscillatory shear (SAOS) and medium amplitude oscillatory shear (MAOS). In the former, the sample measured is subjected to large deformations, which is more reflective of the deformation polymers sustain during most polymer processing techniques; and the analysis is more sensitive to polymer architecture and consequently deformation. LAOS has been used to predict wall slip [8, 9] and polymer morphology, with regards to orientation, during extrusion [10]. Such an approach is a subject of interest for the author, and is currently under investigation.

2.1.2. Filament buckling

An additional consideration with too high a viscosity is filament buckling. The filament acts as the piston that drives the extrusion process. If the filament is not extruded at the desired rate it can apply backpressure to the ensuing filament, and in turn causes it to buckle. A critical stress limit σ_c exists that the filament can be subjected to, of which above this value the filament will buckle, and consequently rendered inadequate. Hence, the critical stress must be greater than the pressure P imparted thereupon to drive the extrusion process.

The pressure required to drive the filament through the nozzle needs to be greater than the filament critical stress by a factor of 1.1 [11], as depicted in **Figure 2**.

The factor of 1.1 accounts for the difference between the nozzle and the filament diameter. The dependence of pressure on viscosity is given in the following equation for an ideal flow:

[2]Typically performed by taking the slope from a double-log plot (i.e. log Viscosity vs log Shear Rate).
[3]Note that since n is between 0 and 1, the true shear rate is greater than the apparent shear rate.

http://dx.doi.org/10.5772/intechopen.77074

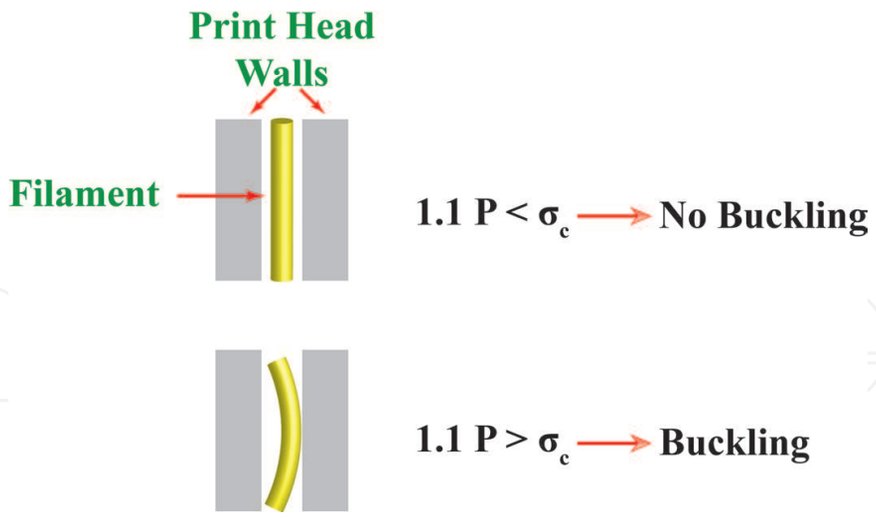


Figure 2. Illustration depicting buckling and no buckling conditions.

$$\mathbf{P} = \frac{2l\eta\,\dot{\gamma}_w}{r} \tag{5}$$

where l is the length of the tube flown through, r is the filament radius, and γ_w is the wall shear rate. Thus, as the pressure is proportional to viscosity and shear rate, reducing the two rheological factors can help mitigate filament buckling; and thereby demonstrating the necessity of rheology once-more.

2.1.3. Further considerations

Prior to extruding, the nozzle is heated to the desired printing temperature, wherein a portion of the filament is housed. The filament should exhibit an appreciable yield strength, whereby flow is resisted at high temperatures until the designated pressure is applied; and thereby preventing 'premature extrusion'. For this reason, the melt should exhibit shear-thinning characteristics at elevated temperatures, whereby the viscosity is high at low shear rates and resists, for example, gravity; but decreases with increasing shear rate. Conversely, a melt with Newtonian flow characteristics possesses no yield strength, and consequently will prematurely extrude, which can result in print failure if not addressed promptly. Therefore, it is necessary to perform viscosity-shear rate measurements and confirm whether the new formulation is shear-thinning in order to avoid premature extrusion.

2.2. Extrudate swelling and viscoelasticity

Extrudate swelling is a frequently encountered phenomenon, and of great interest in polymer processing. The phenomenon occurs in contemporary processes such as hot melt extrusion [12], injection moulding [13] and electrospinning [14], and also reported for fused deposition modelling [15]. Extrudate swell, or die swell, occurs when polymers pass through an orifice with a smaller diameter. The polymer is constrained with energy that is elastically stored as it enters the nozzle, whereafter the energy is released upon exiting the nozzle, leading to a

radial expansion of the melt that consequently results in an extrudate diameter greater than that of the nozzle (**Figure 3**). This event is significant to FDM as it affects print resolution [16]. In addition, it affects print surface topography, which in the case of tissue engineering may influence biological properties. Thus, predicting the degree of extrudate swelling can help to avoid undesirable prints. The size of extrudate swelling is positively affected by shear rate and pressure, and exhibits a negative correlation to temperature and nozzle length. As these are FDM parameters that can be controlled, they can be exploited to minimise extrudate swelling once their effects thereto have been elucidated.

A capillary rheometer is the simplest method of predicting the degree of swelling. The material is extrudate through a capillary die with a similar configuration to that of the FDM nozzle, and the swell ratio B is defined as the ration between extrudate diameter D_{ext} and die diameter D_{die} [17]:

$$B = \frac{D_{ext}}{D_{die}} \tag{6}$$

The swelling phenomenon can also be predicted using a rotational rheometer. Tanner et al. demonstrated that the above equation is correlated to both the wall shear stress and zero-shear viscosity [18]:

$$\frac{D_{ext}}{D_{die}} = \left[1 + \frac{\tau_w^2}{2\,G_0^2}\right]^{1/6} \tag{7}$$

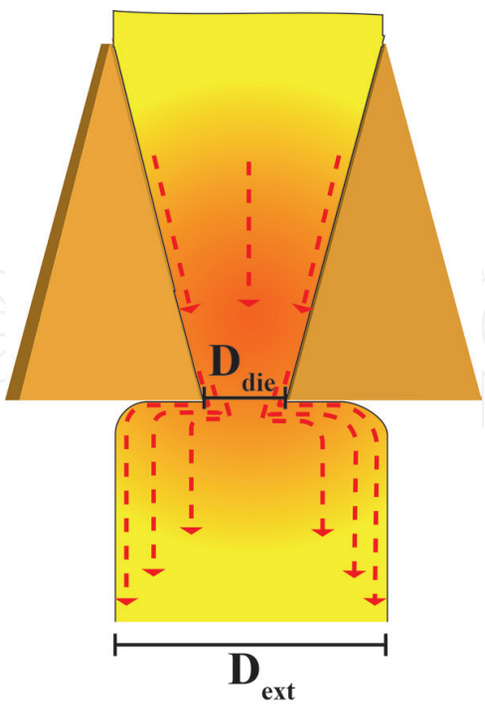


Figure 3. Cross-sectional view of the nozzle portraying extrudate swelling. The schematic illustrates that the extrudate diameter (D_{ext}) is greater than the diameter of the die (or nozzle) (D_{die}) once the melt exits the orifice.

where τ_w is the wall shear stress; and $G_0 = \eta_0/\lambda$, where λ is the relaxation time and η_0 is the zero-shear viscosity. The zero-shear viscosity can be determined by a rheological mathematical model (for example the Williamson or Cross Model) following a viscosity-shear rate test. In a modified FDM, the wall shear stress was acknowledged to induce swelling, and accordingly a lower extrusion speed was opted for to limit extrudate swell [19]. This corresponded with another study that found increasing the extrusion speed increased the filament diameter, again due to extrudate swelling, but also due to time-dependent deformation [20]. Similarly, a slower hot melt extrusion rate is once-more favoured for fabricating filaments suitable for FDM [21], given the latter's low diameter tolerance.

The relaxation time λ is another rheologically-derived parameter that has been proven to correlate well to extrudate swelling. The relaxation time can be obtained through various rheological tests, including from a steady shear rate measurement and curve fitting the data to the Carreau model; or by performing an oscillatory frequency sweep [22, 23]. The relaxation time is directly proportional to the ratio of extrudate swell, therefore, a shorter relaxation time is indicative of improved melt stability and of a polymer that is less susceptible to extrudate swelling [24–27]. Furthermore, the lower the relaxation time in contrast to the deformation time (e.g. time spent deformed in the die or nozzle) then extrudate swelling will be of less concern [13].

2.2.1. Analysing extrudate swelling through creep recovery

Creep and creep recovery experiments are two-halves of an experiment. First, a constant stress σ_0 is applied to the sample and the shear deformation is measured. The stress is then removed at t_1 and the recovery of the deformation is observed in creep recovery. In an elastic material, the strain generated, and the strain recovery is instantaneous to the application and removal of the stress, respectively. However, polymeric materials, which display viscoelastic deformation, convey a different response. Under the constant stress, part of the polymer strains instantly, whereas another part of the polymer deforms at a slower rate under the action of the stress; hence the term 'creep'. Similarly, in the recovery phase, a part of the material recovers instantly, another slowly recovers, and a final part does not recover completely, and hence, the polymer remains permanently deformed [28] (**Figure 4**).

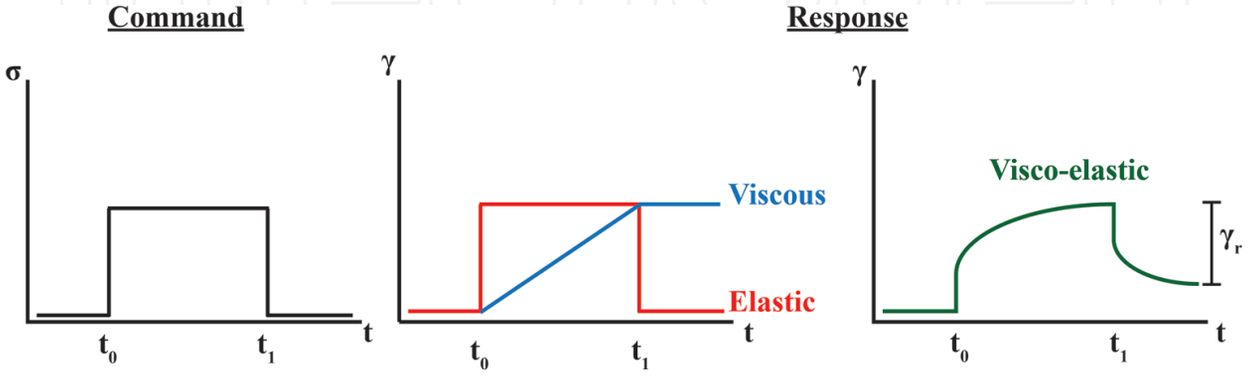


Figure 4. Schematic delineating the possible material responses to a creep test. (t- time; t_0- onset of stress; t_1 _ Endpoint of stress; σ - stress; γ- strain; γ_r recoverable strain).

In the context of extrudate swelling, a creep and creep recovery experiment is analogous to the events that result therein, hence, the test is more closely related to extrudate swell than any other test measurable in a standard rheometer [29]. From a qualitative perspective, a polymer that displays a larger recovery following removal of the stress will indicate a tendency to exhibit a larger extrudate swelling. Conversely, little or no strain recovery is attributed to damping of the applied load [30].

For an experimental quantification in predicting extrudate swelling using a creep recovery test: typically the recoverable compliance J_r is determined, which is positively correlated to extrudate swelling [29, 31, 32]. After the stress is removed, the ratio between recoverable strain γ_r as a function of recovery time t_r, and stress applied σ_0 gives the recoverable compliance [33]:

$$J_r(\sigma_0, t_0, t_r) = \gamma_r(\sigma_0, t_0, t_r)/\sigma_0 \tag{8}$$

2.2.2. Analysing extrudate swelling through stress relaxation

Stress relaxation is another rheological test that can be employed to understand melt viscoelasticity, and verily the effects of stress relaxation characteristics on extrudate swell have been investigated [34–37]. A stress relaxation experiment entails applying a strain to a previously stress-free material and measuring the stress decay at this fixed strain (**Figure 5**). This test is used to determine whether the stress will dissipate within the processing technique time scale. In addition to extrudate swelling, stress relaxation may also help to explain flow warpage[4] [38], and other flow distortions.

Stress relaxation measurements can be made using step-strain rheology. Here, the molten polymer is subjected to an abrupt strain γ at time t_0, typically in the order of 20 ms, and the stress σ needed to keep this deformation is recorded as a function of time [39] (**Figure 5**). The strain applied should be in the linear-viscoelastic region. The relaxation modulus G can be simply determined from this measurement:

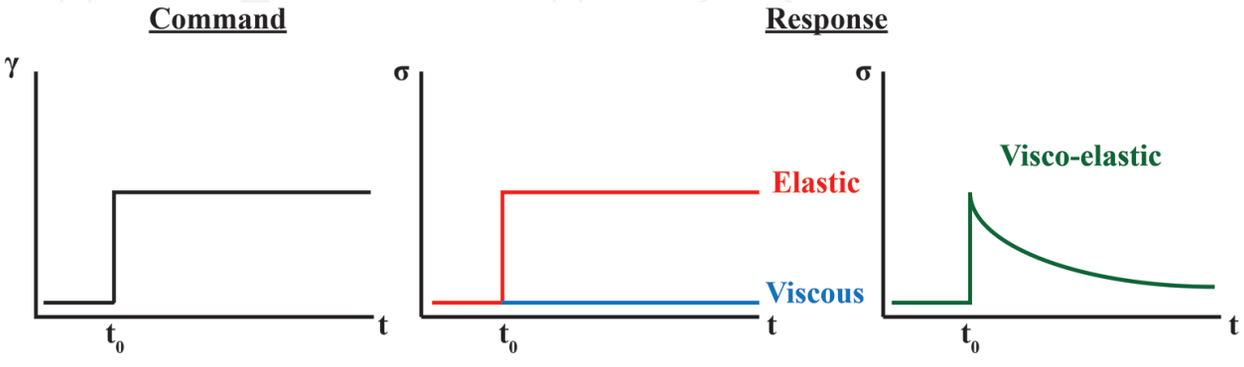


Figure 5. Schematic delineating the stress response to a stress-relaxation test.

[4]This is referred to as 'flow warpage' to differentiate it from 'drying warpage', where the former results in warped (i.e. bent) extrudates; whereas the latter results in a warped print due to inhomogeneous cooling.

http://dx.doi.org/10.5772/intechopen.77074

$$G(t) = \sigma(t)/\gamma \tag{9}$$

Computational studies experimentally determine the relaxation modulus G(t) to obtain the damping function [40–42] for their numerical swell predictions. The damping function has been found to correspond well with swell results empirically determined by a capillary rheometer [34, 43]. Transferring these computational studies, from extrusion dies to FDM nozzles, will indeed enhance FDM productivity. Additionally, determining damping behaviour of polymers is of general interest as it provides insight into the molecular structure thereof [44, 45]; which is not only helpful in understanding polymer behaviour under deformation, and thereby relevant to many fabrication techniques, but also can help in understanding, for example, polymer disintegration in a solvent medium. Therefore, rheological analysis delivers information that will be of interest beyond the FDM processing stage.

2.3. Filament deposition: layer bonding and cooling

The final stage of the FDM process is the layer-by-layer deposition of the filament. In this stage, the first layer is deposited and adheres onto the build platform. Subsequent layers are deposited thereupon, whereby adjacent layers adhere together until the 3D print is completed. The bonding quality determines the final properties of the 3D print; for example, poorly adhered layers exhibit weak mechanical properties. The layer bonding is referred to as sintering, which in polymers is driven by viscous sintering. Hence, viscosity plays another key role at this stage. There are numerical models used for predicting filament coalescence between two layers using viscosity measurements [46, 47], however, depending on the material used or printing parameters, the theoretical model may underestimate the neck growth achieved between adjacent models [48] (**Figure 6**).

Most FDM printers have the option of controlling the temperature of the build platform. Ideally, the temperature should be high enough to ensure that viscous sintering can be achieved, and thereby adhesion. Below a critical sintering temperature sintering is negligible [46]. Equally, the build plate temperature should also ensure that the material possesses sufficient strength to maintain its structural integrity, particularly as layers are deposited above. Thus, a dynamic cooling ramp, via a rotational rheometer, can be utilised to examine the cooling evolution of the newly formulated material, and compared to that of an already successfully printed melt. Such a test can be incorporated to directly follow either a steady- or dynamic-shear test to determine whether shearing influences the solidification process, due to polymer chain dis-entanglement.

Finally, as adherence plays a vital role in FDM, and the printing parameters can affect polymer adhesive properties [49], this presents a potential to perform a tack test. Although not strictly rheology, a tack test allows one to determine the tack, or ‘stickiness’, properties of a material, which can be performed at elevated temperatures on some rotational rheometers. Information such as pull-off force, and mode of failure (i.e. cohesive failure, adhesive failure, or both) can be obtained. Furthermore, a tack test can be preceded by a shearing test, where the effects of shearing on tack properties can be measured [50].

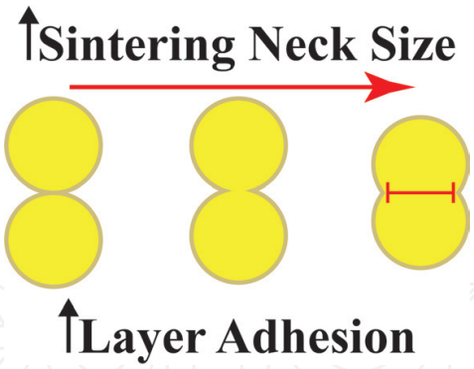


Figure 6. Schematic depicting the evolution of neck size during polymer sintering. The larger the sintering neck size formed the better the adhesion between adjacent layers.

3. Stereolithography

Stereolithography (SLA) is a widely used additive manufacturing technique in the field of polymers, as well as ceramics (**Figure 7**). Here, a monomer resin is polymerised by a laser, layer-by-layer, until a 3D print is fabricated. Hence it differs from fused deposition modelling and other additive manufacturing techniques as it does not involve the use of a nozzle. Such light-curable resins are referred to as photopolymers. In its simplest form, the resin will include the photopolymer and a photoinitiator: the compounds needed to initiate cross-linking of the monomers. However, other additives can be incorporated to modify the properties, such as modifying the mechanical properties of the final product, or the viscosity of the pre-cured resin [51]. Additionally, the resin is a suitable binder for fashioning metal, ceramic and glass materials; and in conjunction with the spatial resolution obtainable, makes SLA an attractive technique for fabricating complex three-dimensional structures.

SLA has been used in the field of structural, tissue engineering, electronics and pneumatically-actuated soft robots [52, 53], and ergo, demonstrating its wide applicability. There are many advantages to this technique over FDM, including printing can be achieved without high temperatures, higher spatial resolution, and nozzle clogging is not of concern. SLA is predominantly Couette flow, thus only rotational rheometry is pertinent here. Furthermore, the dynamic aspect of rotational rheometers can be used for photorheology, which will be described in Section 3.2.

3.1. Viscosity measurements

In comparison to FDM, both the operating viscosity and shear rates are considerably smaller. The viscosity of the photopolymer should be under 5 Pa.s at 30 s^{-1} [54, 55], which ensures that the photopolymer is free-flowing, and capable of forming a new layer (i.e. recoating) ready for polymerisation. However, this value depends on the SLA printer, as others require, for example, a viscosity below 10 Pa.s at 100 s^{-1} [56]. This will ultimately depend on the settings of the SLA printer, but nonetheless, one should consider the maximum operable viscosity prior to printing.

http://dx.doi.org/10.5772/intechopen.77074

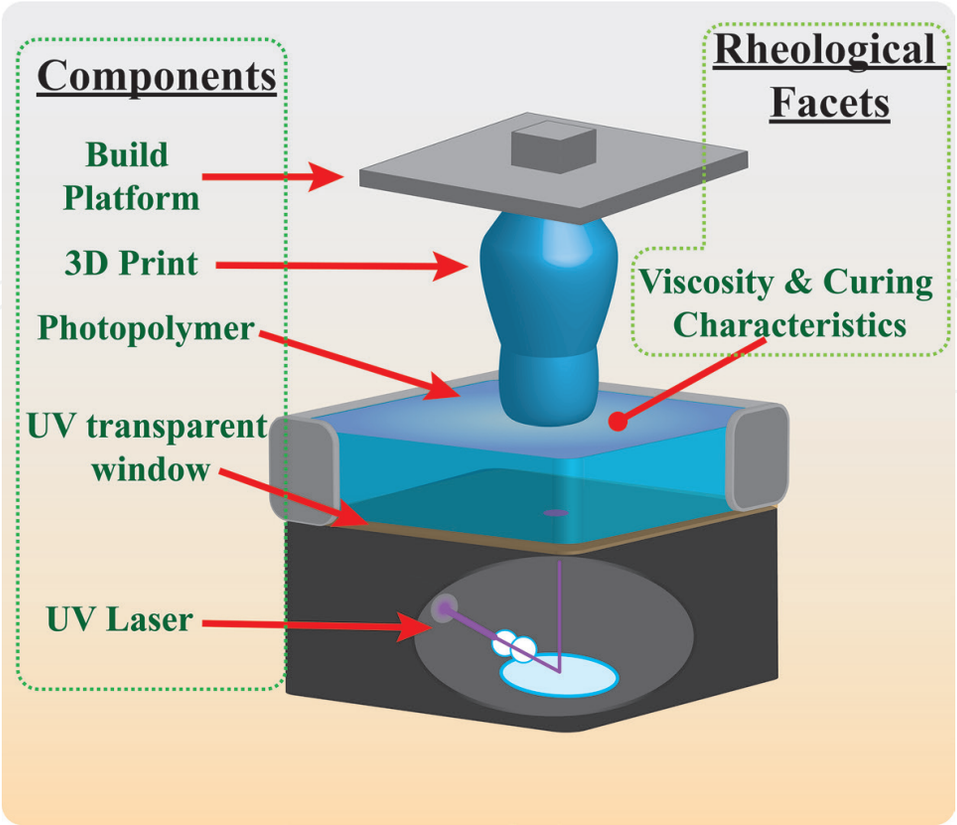


Figure 7. Representative schematic of a stereolithography printer. The figure includes the components that comprise the printer, and the rheological facet of interest.

The viscosity measurement is achieved by performing a steady-shear rate test on the resin free from curable light source(s). The test can be performed at the SLA's functioning shear rate, whether it be 30 s^{-1}, 100 s^{-1} or any other value, and ensuring the viscosity is below the effective threshold[5]; but the test is more commonly performed at a wider shear rate range as more information can be attained. Alternatively, a repeated cycle of LAOS and SAOS can be used; whereby LAOS for reflecting the deformation imparted during the submergence and withdrawal (**Figure 8**); and SAOS to investigate the viscoelastic recovery [57]. At the initial position during SLA printing, the build platform is lowered until submersion thereof is achieved. The platform is thereafter withdrawn, before being submerged again. During withdrawal, the resin should possess a low viscosity to attain complete recoating. Otherwise, a resin with high viscosity, the platform will be lowered with an incomplete recoating. A repeated cycle of LAOS and SAOS can be informative as to whether the structure can recover following deformation by the submersion of the build platform.

Measuring the viscosity over a range of shear rates rather than at a single point would be of particular interest to those formulating a UV-curable suspension, as parameters such as degree of shear-thinning and yield stress are of importance. The yield stress is correlated to the stability

[5]If working with a commercial printer whose supplier produces their own photopolymer resin, then one can measure the viscosity thereof, and attempt to closely match it.

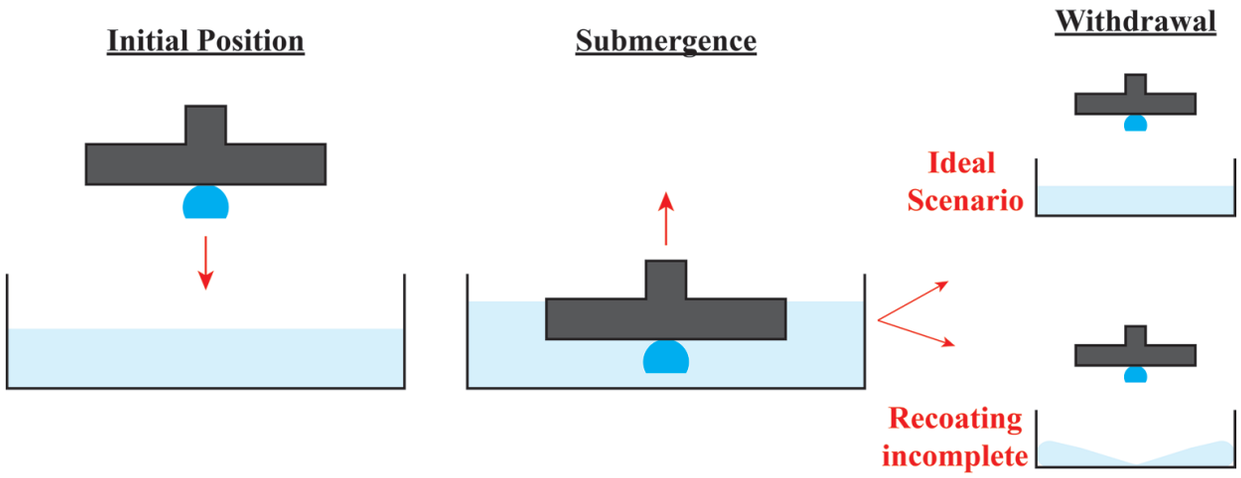


Figure 8. Illustration depicting SLA sequence of events.

of the suspension, which would provide insight into the stability of the suspension over time, and the tendency of the particles to sediment. Particle sedimentation is indeed undesirable as it results in an inhomogeneous print. Other rheological analysis performed to elucidate the degree of sedimentation in suspensions include determining the tan δ from oscillatory tests, creep-recovery tests and stress relaxation tests [58]. Note that if suspensions are to be measured using a rotational rheometer, then one has to use a plate-plate geometry configuration as a cone-plate configuration is susceptible to erroneous measurement due to the particles.

If a UV-curable emulsion has been formulated, and syneresis (i.e. phase separation between the two solvents) is of concern, then a frequency sweep is advisable. Using this test, a storage modulus G' of comparable magnitude, or superior, to the loss modulus G'', at the low frequency (i.e. longer periods) suggests the emulsion is less likely to exhibit syneresis. In other words, a high tan δ indicates a higher tendency to exhibit syneresis [59].

A minimum viscosity limit on the other hand appears to be less discussed, as this is less problematic for most researchers. One author inferred a minimum of 2 Pa.s [55], albeit successful SLA prints were achieved with a viscosity between 0.1 and 1 Pa.s [53, 60].

The low viscosities make SLA desirable as a binder for powder metallurgy, as more of the inorganic powder can be suspended therein. Both metal and ceramic structures have been fabricated using SLA, wherein the inorganic particles are suspended therein; cured into the desirable 3D structure, and subsequently thermally de-bound, leaving behind only the inorganic material [61] elbadawi et al. The material is then sintered to achieve permanence. To achieve a green body that is mechanically sound, at least 40 vol% solids loading is needed, and as expected, this produces a substantial increase in viscosity, above the operating range. However, through the incorporation of dispersants and diluents, the viscosity can be lowered, and hence rheological analysis is key to identifying the minimum dispersant concentration needed to produce a suitable resin.

If working with a photopolymer resin that is not liquid at room temperature, then a viscosity test of importance will be to perform a temperature ramp. Elomaa et al. (2011) opted to

formulate a solvent-free photopolymer comprising of polycaprolactone, in which heating was needed to achieve the operable viscosity [62]. If such an approach is pursued, then performing a temperature ramp will help to identify the minimum temperature without needing to use an unnecessarily high value.

3.2. Photorheology: dynamic mechanical analysis

Aside from viscosity measurement, a rheometer is an indispensable tool for SLA as it can be used to measure the cross-linking characteristic of the resin. As mentioned, the monomer transforms from a liquid to a solid upon UV contact, which can be measured by a rotational rheometer. The transition from resin to solid manifest itself in a tremendous increase to both the storage and loss modulus, with values such as a curing time and material stiffness extracted. This entails the use of an oscillatory time ramp, whereby both the storage and loss modulus are recorded over time (**Figure 9**). The test is allowed to run until a baseline value for the resin is obtained, whereafter a UV source is activated, and the solidification behaviour is observed. Both the time to achieving solidification and the shear modulus of the solid can be quantified. The former is necessary to predict the scanning speed of the UV laser needed to achieve a solid structure; whereas the latter provides a strong correlation to the mechanical properties of the 3D print, namely Young's Modulus [63]. Such a test saves both time and cost.

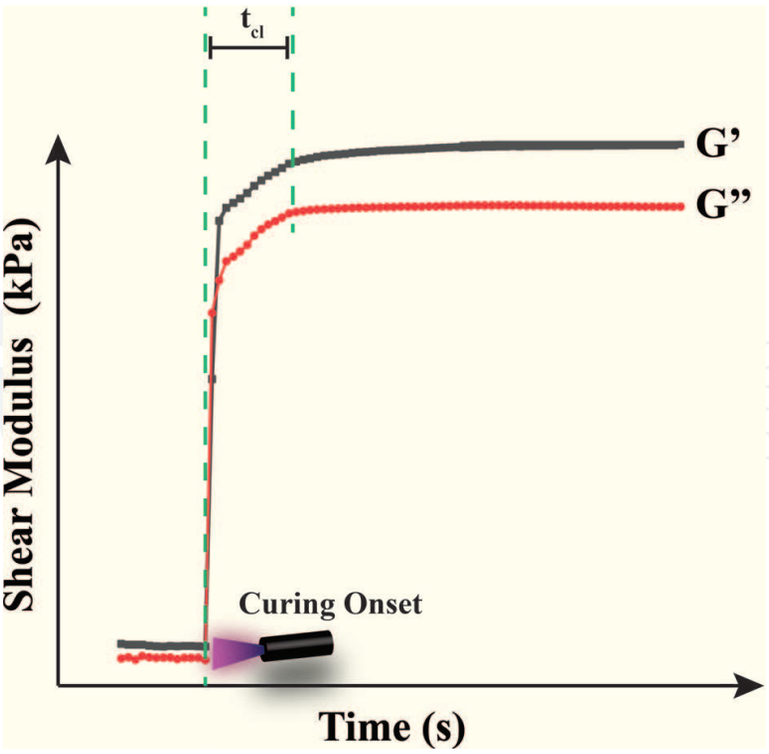


Figure 9. Representative dynamic mechanical analysis curve for measuring the crosslinking characteristics of a UV-curable formulation.

The shrinkage of the material can also be measured by exploiting the rheometer's[6] axial movement, and the upper plate geometry can be adjusted to move in-line with the shrinkage that occurs with cross-linking. As **Figure 10** demonstrates, a minimum compressive force is

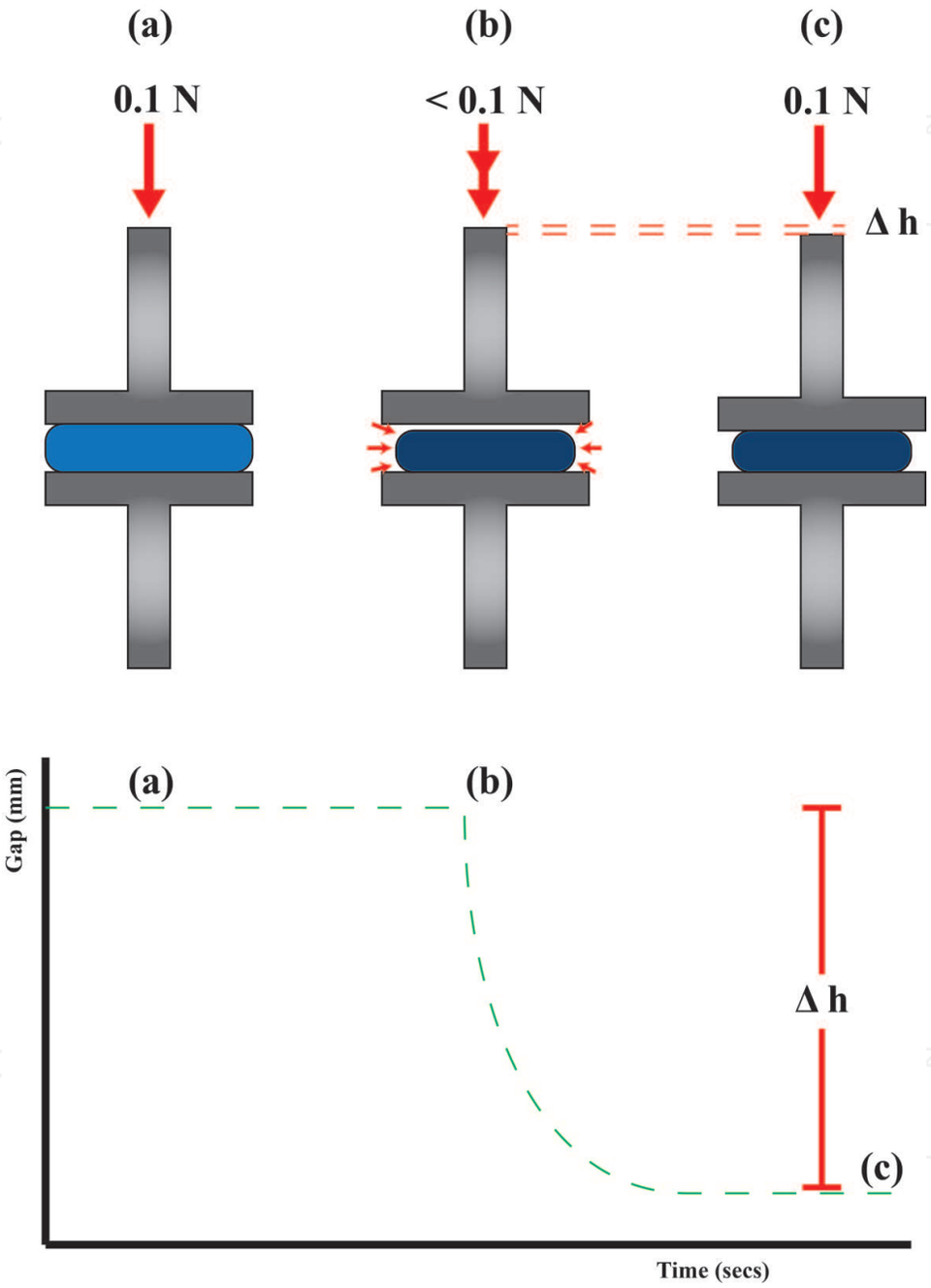


Figure 10. Schematic illustrating the events occurring when measuring shrinkage due to UV-curing. (a) at first the rheometer plate establishes a baseline by applying a prescribed axial force (0.1 N). As the sample is cured it shrinks (b) causing a decrease in the force, and subsequently the rheometer moves axially until the prescribed force is re-established (c). Such movements allow the simultaneous measurement of the gap decrease(Δh).

[6]For Example TA Instruments Discovery Hybrid Series rheometers, which can measure both tensile and compressive forces up to 50 N.

applied to the sample during oscillatory measurements, which if not registered will cause the upper plate to move until the compressive force is re-established. Therefore, in addition to measuring the crosslinking properties of the photopolymers, a rotational rheometer can be incorporated to offer insight into the material's shrinkage characteristics.

4. Other techniques

Given the success and ubiquity of FDM, similar extrusion-based additive manufacturing techniques exists. Examples include bioprinters, where hydrogels and cells are extruded; robocasting, where a ceramic, metallic, or glass powder enveloped by a polymeric binder is extruded; and inkjet printing, where polymeric inks are ejected. Said techniques differ to FDM with respect to their printing conditions. For example, bioprinters and robocasting can be performed at room temperature, and hence high-temperature rheology is of less interest. Another example is the solidification process post-extrusion: where FDM relies in cooling for the material post-extrusion to maintain its structural integrity, cold-extrusion techniques require shear-thinning materials that can rapidly restore their structural integrity following shearing [63]. Moreover, each of the aforementioned techniques have their unique desirable rheological properties, with respect to viscosity ranges, flow characteristics and dynamic mechanical properties. These are just a few of the common extrusion-based AM techniques, and as the field progresses, alternative derivatives are anticipated. Hence, the desirable rheological properties will evolve accordingly, and it is for this reason, that rheology will need to be a habitual characterisation technique in polymer AM fabrication.

A brief mention of selective laser sintering (SLS) is merited. Distinctly different from other techniques, SLS utilises a laser to sinter adjacent polymer powders laterally, such as nylon, and subsequently layer-by-layer to fashion a 3D print. After each layer is fully sintered, a new powder layer is deposited, prior to sintering. The ability of the powder to flow, as well as its packing performance and distribution behaviour, are of interest; and where powder rheology can be employed for elucidation thereof. Measurements performed using a powder rheometer include powder flow, particle-particle interaction during flow, compressibility, and adhesivity. Furthermore, the sintering behaviour discussed in Section 2.3 are applicable herein. Thus, despite SLS possessing a dissimilar mode of operation, rheology is still a relevant technique.

5. Concluding remarks

The chapter has demonstrated the necessity and utility of rheological characterisation techniques for polymer-based additive manufacturing, irrespective of the technique. For fused deposition modelling, rheologically characterisation are performed to obtain the true shear rate at the nozzle wall, the ideal viscosity for material flow, the critical buckling stress, extrudate swelling and sintering characteristics. For stereolithography, a contrasting AM technique, rheology is a requisite for ensuring the resin possesses the ideal viscosity, as well as attaining information regarding the curing characteristics and mechanical properties of the cured resin.

Author details

Mohammed Elbadawi

Address all correspondence to: elbadawi.moe@gmail.com

Pharmaceutical Science and Biomaterials Research Group, Division of Medical Sciences, Department of Health Sciences, Luleå University of Technology, Luleå, Sweden

References

[1] Son Y. Determination of shear viscosity and shear rate from pressure drop and flow rate relationship in a rectangular channel. Polymer (Guildf) [Internet]. 2007;**48**(2):632-637. DOI: 10.1016/j.polymer.2006.11.048

[2] Boetker J, Water JJ, Aho J, Arnfast L, Bohr A, Rantanen J. Modifying release characteristics from 3D printed drug-eluting products. European Journal of Pharmaceutical Sciences. 2016;**90**:47-52. DOI: 10.1016/j.ejps.2016.03.013

[3] Aho J, Boetker JP, Baldursdottir S, Rantanen J. Rheology as a tool for evaluation of melt processability of innovative dosage forms. International Journal of Pharmaceutics [Internet]. 2015;**494**(2):623-642. DOI: 10.1016/j.ijpharm.2015.02.009

[4] Ren X, Shao H, Lin T, Zheng H. 3D gel-printing—An additive manufacturing method for producing complex shape parts. Material Design [Internet]. 2016;**101**:80-87. DOI: 10.1016/j.matdes.2016.03.152

[5] Giovanni P, Gabriele N, Gianmarco G, Marinella L, Stefano T. UV-assisted three-dimensional printing of polymer nanocomposites based on inorganic fillers. Polymer Composition [Internet]. 2017 Aug 8;**38**(8):1662-1670. DOI: 10.1002/pc.23735

[6] Lobe VM, White JL. An experimental study of the influence of carbon black on the rheological properties of a polystyrene melt. Polymer Engineering and Science [Internet]. 2004 Aug 25;**19**(9):617-624. DOI: 10.1002/pen.760190905

[7] Cox WP, Merz EH. Correlation of dynamic and steady flow viscosities. Journal of Polymer Science [Internet]. 1958 Apr 1;**28**(118):619-622. DOI: 10.1002/pol.1958.1202811812

[8] Coblas D, Broboana D, Balan C. Correlation between large amplitude oscillatory shear (LAOS) and steady shear of soft solids at the onset of the fluid rheological behavior. Polymer (Guildf) [Internet]. 2016;**104**:215-226. DOI: 10.1016/j.polymer.2016.06.003

[9] Graham MD. Wall slip and the nonlinear dynamics of large amplitude oscillatory shear flows. Journal of Rheology (N Y N Y) [Internet]. 1995;**39**(4):697-712. DOI: 10.1122/1.550652

[10] Hyun K, Wilhelm M, Klein CO, Cho KS, Nam JG, Ahn KH, et al. A review of nonlinear oscillatory shear tests: Analysis and application of large amplitude oscillatory shear

(LAOS). Progress in Polymer Science [Internet]. 2011;**36**(12):1697-1753. DOI: 10.1016/j.progpolymsci.2011.02.002

[11] Sriram R, Gang Q, Natesan V, Ahmad S, DS C. Powder processing, rheology, and mechanical properties of feedstock for fused deposition of Si_3N_4 ceramics. Journal of American Ceramic Society [Internet]. 2004 Dec 20;**83**(7):1663-1669. DOI: 10.1111/j.1151-2916.2000.tb01446.x

[12] Zhang F, McGinity JW. Properties of sustained-release tablets prepared by hot-melt extrusion. Pharmaceutical Development and Technology [Internet]. 1999 Jan 1;**4**(2):241-250. DOI: 10.1081/PDT-100101358

[13] Smallman RE, Bishop RJ. Chapter 11 - Plastics and Composites BT - Modern Physical Metallurgy and Materials Engineering. 6th ed. Oxford: Butterworth-Heinemann; 1999. pp. 351-375. DOI: 10.1016/B978-075064564-5/50011-2

[14] Diban N, Haimi S, Bolhuis-Versteeg L, Teixeira S, Miettinen S, Poot A, et al. Development and characterization of poly(ε-caprolactone) hollow fiber membranes for vascular tissue engineering. Journal of Membrane Science [Internet]. 2013;**438**:29-37. DOI: 10.1016/j.memsci.2013.03.024

[15] Monzón MD, Gibson I, Benítez AN, Lorenzo L, Hernández PM, Marrero MD. Process and material behavior modeling for a new design of micro-additive fused deposition. International Journal of Advanced Manufacture Technology [Internet]. 2013 Aug;**67**(9):2717-2726. DOI: 10.1007/s00170-012-4686-y

[16] Rimington RP, Capel AJ, Christie SDR, Lewis MP. Biocompatible 3D printed polymers via fused deposition modelling direct C2C12 cellular phenotype in vitro. Lab Chip [Internet]. 2017;**17**(17):2982-2993. DOI: 10.1039/C7LC00577F

[17] Gomes ACO, Soares BG, Oliveira MG, Pessan LA, Paranhos CM. Influence of compatibilizer content on PA/NBR blends properties: Unusual characterization and evaluation methods. Journal of Applied Polymer Science [Internet]. 2013 Feb 5;**127**(3):2192-2200. DOI: 10.1002/app.37792

[18] Tanner RI. A theory of die-swell. Journal of Polymer Science Part A-2 Polymer Physics [Internet]. 1970 Dec 1;**8**(12):2067-2078. DOI: 10.1002/pol.1970.160081203

[19] Lu X, Lee Y, Yang S, Hao Y, Evans JRG, Parini CG. Fine lattice structures fabricated by extrusion freeforming: Process variables. Journal of Material Processing Technology [Internet]. 2009;**209**(10):4654-4661. DOI: 10.1016/j.jmatprotec.2008.11.039

[20] Lu X, Lee Y, Yang S, Hao Y, Evans J, Parini C. Extrusion freeforming of millimeter wave electromagnetic bandgap (EBG) structures. Rapid Prototype Journal [Internet]. 2009 Jan 16;**15**(1):42-51. DOI: 0.1108/13552540910925054

[21] Murphy CA, Collins MN. Microcrystalline cellulose reinforced polylactic acid biocomposite filaments for 3D printing. Polymer Composite [Internet]. 2016 May 1;**n**(a-n):a. DOI: 10.1002/pc.24069

[22] Mackley MR, Marshall RTJ, Smeulders JBAF, Zhao FD. The rheological characterization of polymeric and colloidal fluids. Chemical Engineering Science [Internet]. 1994;**49**(16): 2551-2565. DOI: 10.1016/0009-2509(94)E0082-2

[23] Banerjee SS, Kumar KD, Bhowmick AK. Distinct melt Viscoelastic properties of novel nanostructured and microstructured thermoplastic elastomeric blends from polyamide 6 and fluoroelastomer. Macromolecular Material Engineering [Internet]. **300**(3):283-290. DOI: 10.1002/mame.201400264

[24] Threepopnatkul P, Teppinta W, Sombatsompop N. Effect of co-monomer content on rheological property of sawdust/ABS composites. Advanced Material Research [Internet]. 2010;**93-94**:611-614. DOI: 10.4028/www.scientific.net/AMR.93-94.611

[25] Yang Q, Chung T-S, Weber M, Wollny K. Rheological investigations of linear and hyperbranched polyethersulfone towards their as-spun phase inversion membranes' differences. Polymer (Guildf) [Internet]. 2009;**50**(2):524-533. DOI: 10.1016/j.polymer.2008.11.039

[26] Koopmans RJ. Extrudate swell of high density polyethylene. Part II: Time dependency and effects of cooling and sagging. Polymer Engineering Science [Internet]. 1992 Dec 1;**32**(23):1750-1754. DOI: 10.1002/pen.760322303

[27] Aho J, Boetker J, Baldursdottir S. Rheology as a tool for evaluation of melt processability of innovative dosage forms. International Journal of Pharmaceutics [Internet]. 2015 Oct 30 [cited 2017 Oct 20];**494**(2):623-642. DOI: 10.1016/j.ijpharm.2015.02.009

[28] Münstedt H, Schwarzl FR. Linear viscoelastic deformation behavior in simple shear. In: Deformation and Flow of Polymeric Materials [Internet]. Berlin, Heidelberg: Springer Berlin Heidelberg; 2014. pp. 121-187. DOI: 10.1007/978-3-642-55409-4_5

[29] den Doelder CFJ, Koopmans RJ. The effect of molar mass distribution on extrudate swell of linear polymers. Journal of Nonnewtonian Fluid Mechanics [Internet]. 2008;**152**(1):195-202. DOI: 10.1016/j.jnnfm.2007.04.005

[30] Zheng H, Wang G, Zhou C, Yu W, Zhang H. Computer-aided optimization of the extrusion process of automobile rubber seal. Journal of Macromolecular Science Part A [Internet]. 2007 Mar 1;**44**(5):509-516. DOI: 10.1080/10601320701235552

[31] Münstedt H, Schwarzl FR. Rheological properties and molecular structure. In: Deformation and Flow of Polymeric Materials [Internet]. Berlin, Heidelberg: Springer Berlin Heidelberg; 2014. pp. 419-452. DOI: 10.1007/978-3-642-55409-4_13

[32] Handge UA, Zeiler R, Dijkstra DJ, Meyer H, Altstädt V. On the determination of elastic properties of composites of polycarbonate and multi-wall carbon nanotubes in the melt. Rheologica Acta [internet]. 2011 Jun;**50**(5):503. DOI: 10.1007/s00397-011-0558-x

[33] Münstedt H, Schwarzl FR. Shear rheology. In: Deformation and Flow of Polymeric Materials [Internet]. Berlin, Heidelberg: Springer Berlin Heidelberg; 2014. p. 363-386. ADOI: 10.1007/978-3-642-55409-4_11

[34] Huang SX, Lu CJ. Stress relaxation characteristics and extrudate swell of the IUPAC-LDPE melt. Journal of Nonnewtonian Fluid Mechanics [Internet]. 2006;**136**(2):147-156. DOI: 10.1016/j.jnnfm.2006.03.013

[35] Konaganti VK, Ansari M, Mitsoulis E, Hatzikiriakos SG. The effect of damping function on extrudate swell. Journal of Nonnewtonian Fluid Mechanics [Internet]. 2016;**236**:73-82. DOI: 10.1016/j.jnnfm.2016.08.007

[36] Kiriakidis DG, Park HJ, Mitsoulis E, Vergnes B, Agassant J-F. A study of stress distribution in contraction flows of an LLDPE melt. Journal of Nonnewtonian Fluid Mechanics [Internet]. 1993;**47**:339-356. DOI: 10.1016/0377-0257(93)80057-I

[37] Guillet J, Seriai M. Quantitative evaluation of extrudate swell from viscoelastic properties of polystyrene. Rheologica Acta [Internet]. 1991;**30**(6):540-548. DOI: 10.1007/BF00444372

[38] Rosato D, Rosato D. 2 - Design Optimization BT - Plastics Engineered Product Design. In Amsterdam: Elsevier Science; 2003. pp. 46-160. DOI: 10.1016/B978-185617416-9/50003-X

[39] Kamath VM, Mackley MR. The determination of polymer relaxation moduli and memory functions using integral transforms. Journal of Nonnewtonian Fluid Mechanics [Internet]. 1989;**32**(2):119-144. DOI: 10.1016/0377-0257(89)85032-3

[40] Porter D. Combining molecular and continuum mechanics concepts for constitutive equations of polymer melt flow. Journal of Nonnewtonian Fluid Mechanics [Internet]. 1997;**68**(2):141-152. DOI: 10.1016/S0377-0257(96)01516-9

[41] Garcia-Rejon A, DiRaddo RW, Ryan ME. Effect of die geometry and flow characteristics on viscoelastic annular swell. Journal of Nonnewtonian Fluid Mechanics [Internet]. 1995;**60**(2):107-128. DOI: 10.1016/0377-0257(95)01384-X

[42] Polacco G, Stastna J, Biondi D, Zanzotto L. Relation between polymer architecture and nonlinear viscoelastic behavior of modified asphalts. Current Opinion in Colloidal Interface Science [Internet]. 2006;**11**(4):230-245. DOI: 10.1016/j.cocis.2006.09.001

[43] Ganvir V, Gautham BP, Pol H, Bhamla MS, Sclesi L, Thaokar R, et al. Extrudate swell of linear and branched polyethylenes: ALE simulations and comparison with experiments. Journal of Nonnewtonian Fluid Mechanics [Internet]. 2011;**166**(1):12-24. DOI: 10.1016/j.jnnfm.2010.10.001

[44] Tam KC, Ng WK, Jenkins RD. Non-linear shear deformation of hydrophobically modified polyelectrolyte systems. Polymer (Guildf) [Internet]. 2006;**47**(19):6731-6737. DOI: 10.1016/j.polymer.2006.07.051

[45] Osaki K. On the damping function of shear relaxation modulus for entangled polymers. Rheologica Acta [Internet]. 1993 Sep;**32**(5):429-437. DOI: 10.1007/BF00396173

[46] Bellehumeur C, Li L, Sun Q, Gu P. Modeling of bond formation between polymer filaments in the fused deposition modeling process. Journal of Manufacturing Processes [Internet]. 2004;**6**(2):170-178. DOI: 10.1016/S1526-6125(04)70071-7

[47] Cole DP, Riddick JC, Iftekhar Jaim HM, Strawhecker, KE, Zander NW. Interfacial mechanical behavior of 3D printed ABS. Journal of Applied Polymer Science [Internet]. 2016 Apr;**133**(30):20. DOI: 10.1002/app.43671

[48] Sun Q, Rizvi GM, Bellehumeur CT, Gu P. Effect of processing conditions on the bonding quality of FDM polymer filaments. Rapid Prototype Journal [Internet]. 2008 Mar 28;**14**(2):72-80. DOI: 10.1108/13552540810862028

[49] Hashemi Sanatgar R, Campagne C, Nierstrasz V. Investigation of the adhesion properties of direct 3D printing of polymers and nanocomposites on textiles: Effect of FDM printing process parameters. Applied Surface Science [Internet]. 2017;**403**:551-563. DOI: 10.1016/j.apsusc.2017.01.112

[50] Landa M, Fernandez M, Munoz ME, Santamaria A. The effect of flow on the physical properties of polyurethane/carbon nanotubes nanocomposites: Repercussions on their use as electrically conductive hot-melt adhesives. Polymer Composition [Internet]. 2014 Mar 29;**36**(4):704-712. DOI: 10.1002/pc.22989

[51] Hinczewski C, Corbel S, Chartier T. Stereolithography for the fabrication of ceramic three- dimensional parts. Rapid Prototype Journal [Internet]. 1998 Sep 1;**4**(3):104-111. DOI: 10.1108/13552549810222867

[52] PD K, Hosein SA, Michael L, Biao Z, Qi G, Shlomo M. Highly stretchable and UV curable Elastomers for digital light processing based 3D printing. Advanced Material [Internet]. 2017 Feb 7;**29**(15):1606000. DOI: 10.1002/adma.201606000

[53] Shepherd BNP, TJW, HZ, RF. 3D printing antagonistic systems of artificial muscle using projection stereolithography. Bioinspiration and Biomimetics [Internet]. 2015; **10**(5):55003. DOI: 10.1088/1748-3190/10/5/055003

[54] Wu H, Cheng Y, Liu W, He R, Zhou M, Wu S, et al. Effect of the particle size and the debinding process on the density of alumina ceramics fabricated by 3D printing based on stereolithography. Ceramics International [Internet]. 2016;**42**(15):17290-17294. DOI: 10.1016/j.ceramint.2016.08.024

[55] Thavornyutikarn B, Tesavibul P, Sitthiseripratip K, Chatarapanich N, Feltis B, Wright PFA, et al. Porous 45S5 bioglass®-based scaffolds using stereolithography: Effect of partial pre-sintering on structural and mechanical properties of scaffolds. Materials Science and Engineering: C. 2017;**75**:1281-1288. DOI: 10.1016/j.msec.2017.03.001

[56] Hsiao LC, Badruddoza AZM, Cheng L-C, Doyle PS. 3D printing of self-assembling thermoresponsive nanoemulsions into hierarchical mesostructured hydrogels. Soft Matter [Internet]. 2017;**13**(5):921-929. DOI: 10.1039/C6SM02208A

[57] Faers MA, Choudhury TH, Lau B, McAllister K, Luckham PF. Syneresis and rheology of weak colloidal particle gels. Colloids Surfaces A Physicochemical Engineering Aspects [Internet]. 2006;**288**(1):170-179. DOI: 10.1016/j.colsurfa.2006.03.031

[58] van Vliet T, van Dijk HJM, Zoon P, Walstra P. Relation between syneresis and rheological properties of particle gels. Colloidal Polymer Science [Internet]. 1991 Jun;**269**(6):620-627. DOI: 10.1007/BF00659917

[59] Esposito CC, Mariaenrica F, Domenico A. Rheological characterization of UV-curable epoxy systems: Effects of o-Boehmite nanofillers and a hyperbranched polymeric modifier. Journal of Applied Polymer Science [Internet]. 2009 Jan 30;**112**(3):1302-1310. DOI: 10.1002/app.29603

[60] Elbadawi M, Meredith J, Hopkins L, Reaney I. Progress in bioactive metal and, ceramic implants for load- bearing application. Advanced Techniques in Bone Regeneration [Internet]. Chapter 10. 2016 Aug 31:195-219. DOI: 10.5772/62598

[61] Elomaa L, Teixeira S, Hakala R, Korhonen H, Grijpma DW, Seppälä JV. Preparation of poly(ε-caprolactone)-based tissue engineering scaffolds by stereolithography. Acta Biomaterilia [Internet]. 2011;**7**(11):3850-3856. DOI: 10.1016/j.actbio.2011.06.039

[62] Killion JA, Geever LM, Devine DM, Kennedy JE, Higginbotham CL. Mechanical properties and thermal behaviour of PEGDMA hydrogels for potential bone regeneration application. Journal of Mechanical Behavior of Biomedical Materials [Internet]. 2011;**4**(7):1219-1227. DOI: 10.1016/j.jmbbm.2011.04.004

[63] Elbadawi M, Mosalagae M, Reaney IM, Meredith J. Guar gum: A novel binder for ceramic extrusion. Ceramics International. 2017;**43**:16727-16735. DOI: 10.1016/j.ceramint.2017.09.066

IntechOpen

IntechOpen

IntechOpen